Exact strong zero modes in quantum circuits and spin chains with non-diagonal boundary conditions

Sascha Gehrmann and Fabian H.L. Essler,

The Rudolf Peierls Centre for Theoretical Physics,
Oxford University, Oxford OX1 3PU, UK

arXiv:2511.05490v2 [cond-mat.stat-mech] 10 Nov 2025

Abstract

We construct exact strong zero mode operators (ESZM) in integrable quantum circuits and the spin-1/2 XXZ chain for general open boundary conditions, which break the bulk U(1) symmetry of the time evolution operators. We show that the ESZM is localized around one of the boundaries and induces infinite boundary coherence times. Finally, we prove that the ESZM becomes spatially non-local under the map that relates the spin-1/2 XXZ chain to the asymmetric simple exclusion process, which suggests that it does not play a significant role in the dynamics of the latter.

Contents

1 Introduction **2**

2 Integrable brick-wall circuit with non-diagonal boundary conditions **3**
2.1 Integrability 4
2.2 Exact strong zero mode operator 6
2.2.1 Spatial structure of the ESZM operator 7

3 The spin-1/2 Heisenberg XXZ model **9**
3.1 Infinite edge coherence times 10

4 The asymmetric exclusion process **11**

5 Conclusions **14**

A Explicit matrix elements of the SZM as MPO **15**

B Normalisation Constant for Finite system sizes **16**

C Diagonalisation of $\tilde{\mathcal{A}}$ **17**

References **17**

1 Introduction

Stable edge modes in interacting many-particle systems have attracted a great deal of attention in recent years. For example, they have been known to occur in the ground state sector of models exhibiting topological order [1, 2] for some time. More recently stable, or very long-lived, edge modes have been found at arbitrary energy densities in a range of models [3–8]. These strong zero mode (SZM) operators have interesting physical implications such as long coherence times of spins near the boundaries [9, 10]. Similar edge modes can occur in periodically driven systems [11–20], stochastic processes [21] and interfaces between different phases [22]. Interestingly these modes display a certain degree of robustness under perturbations [9, 23, 24] even though they affect the physical behaviour at finite energy densities. A useful definition of an SZM operator $\overline{\Psi}$ for a many-particle system with Hamiltonian H is [25]

- SZM1: $\|[H, \overline{\Psi}]\| = \mathcal{O}(e^{-\alpha L})$ as $L \to \infty$.
- SZM2: For some operator D generating a discrete symmetry, $[\overline{\Psi}, D] \neq 0$.
- SZM3: $\overline{\Psi}^n \propto \mathbb{1}$ as $L \to \infty$ for some integer $n > 1$.

As was noted in Ref. [5], it is possible to turn a SZM into an exact symmetry by changing the boundary conditions on one of the edges. This gives rise to an exact strong zero mode (ESZM) operator Ψ

$$[\Psi, H] = 0 \ , \tag{1}$$

which is localized in the vicinity of one of the boundaries. So far the analysis of SZM and ESZM operators in the literature has been restricted to boundary conditions which respect global $\mathbb{Z}_2$ or $U(1)$ symmetries of the Hamiltonian. The aim of our work is to prove that this is not required for ESZM operators to exist. The picture that will emerge is most easily explained for the spin-1/2 XXZ Hamiltonian

$$\mathbb{H}_{\mathrm{XXZ}} = \sum_{j=1}^{N-1} \sigma_j^x \sigma_{j+1}^x + \sigma_j^y \sigma_{j+1}^y + \Delta \sigma_j^z \sigma_{j+1}^z + \vec{h}_1 \cdot \vec{\boldsymbol{\sigma}}_1 + \vec{h}_N \cdot \vec{\boldsymbol{\sigma}}_N \ , \qquad \Delta > 1. \tag{2}$$

In the following we show that an ESZM operator localized around the left boundary ($j = 1$) exists as long as we have

$$h_1^z = 0 \ . \tag{3}$$

This can be placed in the general SZM framework as follows. The bulk part of $\mathbb{H}_{\mathrm{XXZ}}$ has a global $U(1) \otimes \mathbb{Z}_2$ symmetry corresponding to arbitrary rotations around the z-axis in spin space, and rotations $R_{\vec{n}}(\pi)$ by π around any axis $\vec{n}$ in the $x - y$ plane. An ESZM operator Ψ exists as long as the left boundary magnetic field $\vec{h}_1$ does not remove the discrete $\mathbb{Z}_2$ symmetry. This requires $\vec{h}_1$ to lie in the x-y plane and the $\mathbb{Z}_2$ symmetry then corresponds to $R_{\vec{h}_1}(\pi)$. The magnetic field $\vec{h}_L$ at the right boundary is allowed to be arbitrary, which is expected on physical grounds: as long as the ESZM operator is localized in the vicinity of the left boundary, the field at the far-away right boundary is not expected to affect it significantly. Constructing a SZM operator $\overline{\Psi}$ from Ψ along the lines of [5, 26] we then have

$$[\overline{\Psi}, R_{\vec{n}}(\pi)] \neq 0 \ , \tag{4}$$

thus fulfilling condition SZM2. The boundary conditions compatible with the existence of an ESZM operator are summarized in Fig.1. Analogous considerations apply in the periodically driven case.

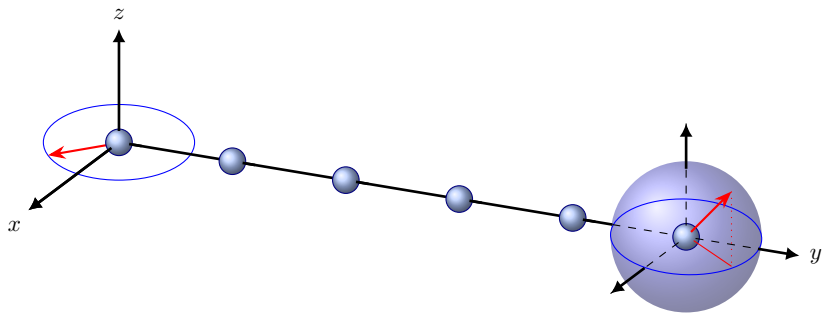

Figure 1: Allowed directions for the boundary magnetic fields $\vec{h}_{1,N}$ (red vectors) in (37) for an ESZM to exist. Black vectors denote the directions in spin space. The U(1) symmetry of the Hamiltonian under rotations around the z-axis is generally broken by these boundary terms.

The outline of this manuscript is as follows. In section 2 we construct a brick-wall quantum circuit with boundary conditions that break the $U(1)$ symmetry of the bulk circuit. The model generalizes the integrable circuit obtained by trotterizing the XXZ Heisenberg spin chain [27–34] (which corresponds to the diagonal-diagonal transfer matrix of the six-vertex model [35,36]) to general open boundary conditions and has the attractive feature of being readily simulable on quantum computers [37–39]. We then show that for a subset of the most general boundary conditions the model exhibits an ESZM. In section 3 we take the Trotter limit to establish the corresponding result for the spin-1/2 Heisenberg XXZ chain. We show that, as expected, the ESZM operator induces infinite edge coherence times for observables that have finite overlaps with the ESZM operator. In section 4 we explore the relation between the spin-1/2 XXZ chain and the asymmetric exclusion process to investigate whether the existence of an ESZ in the former has physically significant implications for the latter. Finally, in section 5 we summarize our results and comment on further developments.

2 Integrable brick-wall circuit with non-diagonal boundary conditions

We start by considering a binary-drive Floquet lattice system consisting of an even number N qubits. The initial state $|\psi_0\rangle$ evolves as

$$|\psi_t\rangle = U^t|\psi_0\rangle \ , \tag{5}$$

where the time-evolution operator takes the form of a brick-wall circuit, *cf.* Fig. 2

$$\begin{aligned} U &= U_{\text{odd}}\, U_{\text{even}}, \\ U_{\text{even}} &= V_1\, V_{2,3}\, \ldots\, V_{N-2,N-1}\, V_N, \\ U_{\text{odd}} &= V_{1,2}\, V_{3,4}\, \ldots\, V_{N-1,N}. \end{aligned} \tag{6}$$

Here, each $V_{j,j+1}$ denotes a local two-qubit unitary gate acting on neighbouring sites $(j, j+1)$, while single-site unitary gates V_j are applied at the edges. We now choose the 2-qbit gates $V_{j,j+1}$ to correspond to the integrable quantum circuit studied in Refs [27–34, 37–39]

$$V_{1,2} = \mathrm{e}^{-\frac{\mathrm{i}\tau}{4}(\sigma_1^x\sigma_2^x+\sigma_1^y\sigma_2^y+\tilde{\Delta}(\sigma_1^z\sigma_2^z-\mathbb{1}))} \ . \tag{7}$$

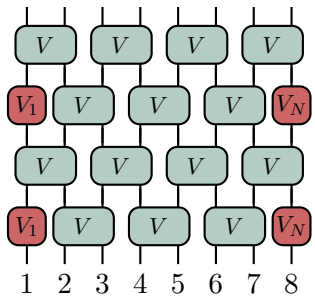

Figure 2: Schematic illustration of the quantum circuits analyzed in this study. The vertical direction represents the progression of time, with the bottom (top) lines denoting the input (output) degrees of freedom. Each full cycle of evolution comprises two successive time layers: during the first, two-qubit gates act on pairs of sites $(2j, 2j+1)$, and during the second, on pairs $(2j+1, 2j+2)$. Red boxes represent boundary one qubit gates. The example shown corresponds to a chain of $N = 8$ qubits evolved for two cycles.

The most general form for the single qubit gates compatible with integrability is

$$V_1 = \mathrm{e}^{\mathrm{i}\boldsymbol{\ell}\cdot\boldsymbol{\sigma}_1} \ , \qquad V_N = \mathrm{e}^{\mathrm{i}\boldsymbol{r}\cdot\boldsymbol{\sigma}_N} \ , \tag{8}$$

where $\boldsymbol{\ell}$ and $\boldsymbol{r}$ are real vectors. In the following we will impose a restriction on $\vec{\ell}$ in order to ensure the existence of an ESZM.

2.1 Integrability

The time evolution operator of the Floquet circuit defined above is equivalent diagonal-to-diagonal transfer matrix of the six-vertex model, which in turn can be viewed as a particular case of the inhomogeneous row-to-row transfer matrix [35]. These observations allow one to bring integrability methods for spin chains with open boundaries to bear [40, 41]. The two-qubit gates can be cast in the form

$$V_{12} = P_{1,2} R_{1,2}(\mathrm{i}\delta) \ , \tag{9}$$

where $\delta \in [0, 2\pi]$, $P_{1,2}$ is the permutation operator, and $R_{1,2}$ is the R-matrix of the XXZ model [42]

$$\begin{aligned} R_{1,2}(u) =& \frac{\sinh(u+\frac{\eta}{2})}{\sinh(u+\eta)} \cosh(\tfrac{\eta}{2})\, \sigma_1^0\, \sigma_2^0 + \frac{\cosh(u+\frac{\eta}{2})}{\sinh(u+\eta)} \sinh(\tfrac{\eta}{2})\, \sigma_1^z\, \sigma_2^z \\ &+ \frac{\sinh(\eta)}{2\sinh(u+\eta)} \big(\sigma_1^x \sigma_2^x + \sigma_1^y \sigma_2^y\big) \ . \end{aligned} \tag{10}$$

Here $\sigma_n^0 = \mathbb{1}_n$ and the parameters η and δ are related to the ones defining our circuit (7) by [31]

$$\cosh\eta = \frac{\sin(\frac{\tilde{\Delta}\tau}{2})}{\sin(\frac{\tau}{2})} \ , \qquad \sin(\delta) = -\sinh(\eta)\tan(\tfrac{\tau}{2}) \ . \tag{11}$$

The single qubit gates (8) are represented in terms of so-called boundary K-matrices, which are solutions to the reflection equations [43]. The most general form appropriate for the unitary circuit 2 is

$$V_1 = \mathrm{Tr}_0\Big(K_0^{(L)}(\tfrac{\mathrm{i}\delta}{2}) V_{0,1}\Big) \ , \qquad V_N = K_N^{(R)}(\tfrac{\mathrm{i}\delta}{2}) \ , \tag{12}$$

where [41]

$$K_a^{(R)}(u) = \frac{1}{\sqrt{c_L}} K_a(u;\, \xi^{(R)}, s^{(R)} e^{\mathrm{i}\varphi^{(R)}}) \ , \quad K_a^{(L)}(u) = \frac{1}{\sqrt{c_R}} K_a(u+\eta; \xi^{(L)}, s^{(L)} \mathrm{e}^{\mathrm{i}\varphi^{(L)}}) \ ,$$
$$K_a(u;\xi,z) = \sinh(2u)\big(z\sigma_a^+ \pm z^*\sigma_a^-\big) + \sinh(u)\cosh(\xi)\sigma_a^z + \cosh(u)\sinh(\xi)\sigma_a^0. \tag{13}$$

The real parameters $\boldsymbol{\ell}$ and $\boldsymbol{r}$ characterizing the quantum circuit in Eq. (8) are obtained by an appropriate choice of $\xi^{(R)}$, $s^{(R,L)}$, and $\varphi^{(R,L)}$. However, to ensure unitary time evolution $V_1 V_1^\dagger = \mathbb{1}_1$, $V_N V_N^\dagger = \mathbb{1}_N$ we have the following constraints. The imaginary part of the ξ's is fixed to be an integer or half-integer multiple of π. Further, the $+/-$ sign must be chosen if $\Im m(\xi^{(\cdot)}/\pi)$ is an integer or half-integer respectively. The u-independent constants $c_{L,R}$ are normalization factors given by

$$\begin{aligned} c_L =& -\frac{1}{2}\frac{\cos(2\delta)-\cos(4\eta)}{\sin(\delta-\mathrm{i}\eta)\sin(\delta+\mathrm{i}\eta)}\Big(\big(s^{(L)}\big)^2\sin^2(\delta) + \sin(\tfrac{\delta}{2}-\mathrm{i}\xi^{(L)})\sin(\tfrac{\delta}{2}+\mathrm{i}(\xi^{(L)})^*)\Big)\,, \\ c_R =& \big(s^{(R)}\big)^2\sin^2(\delta) + \sin\big(\tfrac{\delta}{2}-\mathrm{i}\xi^{(R)}\big)\sin\big(\tfrac{\delta}{2}+\mathrm{i}(\xi^{(R)})^*\big)\,. \end{aligned} \tag{14}$$

The transfer matrix of the inhomogeneous six-vertex model obtained from the R-matrix (10) and boundary K-matrices (13) is [40]

$$\begin{aligned} \mathbb{T}\big(u, \tfrac{\mathrm{i}\delta}{2}\big) = \mathrm{Tr}_0\Big[& K_0^{(L)}(u) R_{0,1}(u-\tfrac{\mathrm{i}\delta}{2})\, R_{0,2}(u+\tfrac{\mathrm{i}\delta}{2}) \ldots R_{0,N}(u+\tfrac{\mathrm{i}\delta}{2}) \\ & \times K_0^{(R)}(u)\, R_{N,0}(u-\tfrac{\mathrm{i}\delta}{2})\, R_{N-1,0}(u+\tfrac{\mathrm{i}\delta}{2}) \ldots R_{1,0}(u+\tfrac{\mathrm{i}\delta}{2})\Big]\,. \end{aligned} \tag{15}$$

The transfer matrices defined in this way form a commuting family

$$\Big[\mathbb{T}\big(u, \tfrac{\mathrm{i}\delta}{2}\big), \mathbb{T}\big(v, \tfrac{\mathrm{i}\delta}{2}\big)\Big] = 0\,. \tag{16}$$

Expanding $\mathbb{T}\big(v, \frac{\mathrm{i}\delta}{2}\big)$ around $v=0$ generates a set of conserved, mutually compatible charges $\mathbb{Q}^{(n)}$ with spatially local densities. The transfer matrix can be represented graphically as shown in Fig. 3. Its geometry is by construction identically to the one of our Floquet

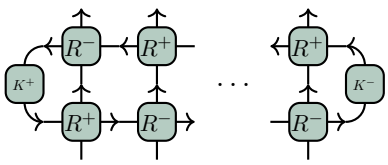

Figure 3: Graphical representation of the double row-to-row transfer matrix. We used the short hand notation $R^\pm = R(u \pm \frac{\mathrm{i}\delta}{2})$.

time-evolution operator and it is easy to see that the two are related by

$$U = \mathbb{T}\big(\tfrac{\mathrm{i}\delta}{2}, \tfrac{\mathrm{i}\delta}{2}\big)\ . \tag{17}$$

This in turn ensures that the conservation laws $\mathbb{Q}^{(n)}$ obtained from the expansion of the transfer matrix around $u=0$ are conserved under time evolution in our Floquet circuit. Their existence precludes the time-evolving state from heating to infinite temperature [44–46], and instead leads to convergence to a generalized Gibbs ensemble [47, 48].

2.2 Exact strong zero mode operator

We now follow Refs [26, 34, 49] and construct a conserved charge from $\mathbb{T}(u)$, which is spatially localized around the left boundary. As we will see, this requires us to fix the parameter $\xi^{(L)}$. The three main steps in the construction are:

- We seek a conserved charge of the form $\mathbb{\Psi} = \mathcal{N}^{-\frac{1}{2}}\mathbb{T}'(u^*)$, where $\mathcal{N}$ is a normalization factor that is chosen such that the Hilbert-Schmidt norm of $\mathbb{\Psi}$ equals 1.
- The parameter u^* is fixed by the requirement

$$R_{0,n}(u^* \pm \tfrac{\mathrm{i}\delta}{2})K_0^{(R)}(u^*)R_{n,0}(u^* \mp \tfrac{\mathrm{i}\delta}{2}) = \text{const } K_0^{(R)}(u^*). \tag{18}$$

  This can be represented graphically as

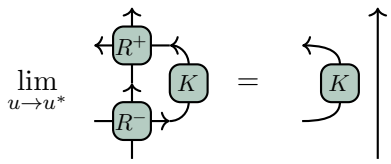

  where $K = K_0^{(R)}(u^*)$ and $R^{\pm} = R_{0,n}(u \pm \frac{\mathrm{i}\delta}{2})$. If (18) is fulfilled then we have

$$\mathbb{\Psi} = \sum_{j=1}^{N} \Psi_j \ , \tag{19}$$

  where the operators Ψ_j act non-trivially only on sites $1, 2, \ldots, j$. In our case the special value for u^* is

$$u^* = \tfrac{\mathrm{i}\pi}{2} \ , \quad K_0^{(R)}(\tfrac{\mathrm{i}\pi}{2}) \propto \sigma_0^z \ . \tag{20}$$

- The parameters associated with the left boundary are chosen such that

$$\lim_{N\to\infty} \|\Psi_j\|^2 \propto e^{-\alpha j} \ , \alpha > 0 \ , \qquad \text{for} \quad j \gg 1, \tag{21}$$

  where $\|.\|$ denotes the Hilbert-Schmidt norm

$$\|\mathcal{O}\|^2 = \tfrac{1}{2^N}\mathrm{Tr}\big(\mathcal{O}^\dagger\mathcal{O}\big) \, . \tag{22}$$

  This ensures that $\mathbb{\Psi}$ is exponentially localized around the left boundary. This requirement forces us to fix $\xi^{(L)}$

$$\xi^{(L)} = \frac{\mathrm{i}\pi}{2} \ . \tag{23}$$

Following Refs [26, 34, 49] we can express the operator defined in this way in a convenient way using matrix-product operators (MPO) $A^{\pm}$

$$\begin{aligned}\mathbb{\Psi} =& \mathcal{N}^{-\frac{1}{2}} B^{(L)}_{\alpha_0} \big[A^+\big]^{\rho_1}_{\alpha_0,\alpha_1} [A^-]^{\rho_2}_{\alpha_1,\alpha_2} \ldots [A^+]^{\rho_{N-1}}_{\alpha_{N-2},\alpha_{N-1}} \big[A^-\big]^{\rho_N}_{\alpha_{N-1}\alpha_N} B^{(R)}_{\alpha_N} \\ & \times \sigma_1^{\rho_1}\sigma_2^{\rho_2} \ldots \sigma_N^{\rho_N} \ .\end{aligned} \tag{24}$$

Here the indices $\alpha_j, \rho_k \in \{0, x, y, z\}$ are summed over. The thermodynamic limit form of $\mathcal{N}$ is (see Appendix B for the finite-volume expression)

$$\mathcal{N}_\infty \equiv \lim_{N\to\infty} \mathcal{N} = 4\big(1 + 4\big(s^{(L)}\big)^2\big)\cosh^2(\eta)\cosh^2(\xi^{(R)}) \, . \tag{25}$$

Explicit expressions for the MPOs $\big[A^{\pm}\big]^{\rho_j}$ and boundary vectors $B^{(R,L)}$ are given in Appendix A.

2.2.1 Spatial structure of the ESZM operator

The representation (24) allows us to obtain MPO expressions for the operators (19)

$$
\begin{aligned}
\Psi_{2j-1} =& \mathcal{N}^{-\frac{1}{2}} B^{(L)}_{\tilde{\alpha}_0} \left[A^+\right]^{\rho_1}_{\tilde{\alpha}_0,\tilde{\alpha}_1} \dots \left[A^-\right]^{\rho_{2j-2}}_{\tilde{\alpha}_{2j-3},\tilde{\alpha}_{2j-2}} \left[A^+\right]^{r_{2j-1}}_{\tilde{\alpha}_{2j-2},\alpha_{2j-1}} \left(\left[A^-\right]^0_{\alpha_{2j-1},\alpha_{2j-1}}\right)^{\frac{N-2j}{2}} \\
&\times \left(\left[A^+\right]^0_{\alpha_{2j-1}\alpha_{2j-1}}\right)^{\frac{N-2j}{2}-1} B^{(R)}_{\alpha_{2j-1}} \, \sigma_1^{\rho_1}\sigma_2^{\rho_2}\dots\sigma_{2j-2}^{\rho_{2j-2}}\sigma_{2j-1}^{r_{2j-1}} \,, \\
\Psi_{2j} =& \mathcal{N}^{-\frac{1}{2}} B^{(L)}_{\tilde{\alpha}_0} \left[A^+\right]^{\rho_1}_{\tilde{\alpha}_0,\tilde{\alpha}_1} \dots \left[A^+\right]^{\rho_{2j-1}}_{\tilde{\alpha}_{2j-2},\tilde{\alpha}_{2j-1}} \left[A^-\right]^{r_{2j}}_{\tilde{\alpha}_{2j-1},\alpha_{2j}} \left(\left[A^+\right]^0_{\alpha_{2j},\alpha_{2j}}\right)^{\frac{N-2j}{2}} \\
&\times \left(\left[A^-\right]^0_{\alpha_{2j}\alpha_{2j}}\right)^{\frac{N-2j}{2}} B^{(R)}_{\alpha_{2j}} \, \sigma_1^{\rho_1}\sigma_2^{\rho_2}\dots\sigma_{2j-1}^{\rho_{2j-1}}\sigma_{2j}^{r_{2j}} \,,
\end{aligned}
\tag{26}
$$

where the tilded indices $\tilde{\alpha}_\ell$ just take the values $0, x, y$, $r_{2j-1}, r_{2j} \in \{x, y, z\}$ and repeated indices are summed over. We note that here the MPOs reduce to 3×3 matrices. As the ESZM operator is localized around the left boundary we provide explicit expressions for $\Psi_{1,2}$

$$
\begin{aligned}
\lim_{N\to\infty} \Psi_1 =& c_{\Psi_1}\Big(\sigma_1^z + 2s^{(L)}\sin(\tfrac{\delta}{2})(\cos(\varphi^{(L)})\sigma_1^x - \sin(\varphi^{(L)})\sigma_1^y)\Big) \,, \\
\lim_{N\to\infty} \Psi_2 =& c_{\Psi_2}\Big(\sigma_2^z - 2s^{(L)}\sin(\tfrac{\delta}{2})\cosh(\eta)\Big(\cos(\varphi^{(L)})\sigma_2^x - \sin(\varphi^{(L)})\sigma_2^y\Big) \\
&+ s^{(L)}\sinh(2\eta)\sec\left(\tfrac{\delta}{2}\right)\Big(\sin(\varphi^{(L)})\sigma_1^x\sigma_2^z + \cos(\varphi^{(L)})\sigma_1^y\sigma_2^z\Big) \\
&+ 2s^{(L)}\sinh(\eta)\sin\left(\tfrac{\delta}{2}\right)\tan\left(\tfrac{\delta}{2}\right)\Big(\sin(\varphi^{(L)})\sigma_1^z\sigma_2^x + \cos(\varphi^{(L)})\sigma_1^z\sigma_2^y\Big) \\
&- \sinh(\eta)\tan\left(\tfrac{\delta}{2}\right)(\sigma_1^x\sigma_2^y - \sigma_1^y\sigma_2^x)\Big) \,,
\end{aligned}
\tag{27}
$$

where

$$
c_{\Psi_1} = \mathcal{N}_\infty^{-\frac{1}{2}} \frac{2\sinh^2(\eta)\cosh(\xi^R)\cosh(\eta)}{\mathrm{i}\,\cosh(\eta - \frac{\mathrm{i}\delta}{2})\cosh(\eta + \frac{\mathrm{i}\delta}{2})} \,, \qquad c_{\Psi_2} = c_{\Psi_1}\frac{\cos^2\left(\frac{\delta}{2}\right)}{\cosh(\eta - \frac{\mathrm{i}\delta}{2})\cosh(\eta + \frac{\mathrm{i}\delta}{2})} \,. \tag{28}
$$

In order to prove that the ESZM operator Ψ is localized around the left boundary we now consider the Hilbert-Schmidt norm of the Ψ_j

$$
\|\Psi_j\|^2 = \frac{1}{2^N}\mathrm{Tr}\big(\Psi_j^\dagger\Psi_j\big) \,, \tag{29}
$$

and show that these decay exponentially in j (for large j). These norms can be calculated analytically by employing an MPO representation

$\|\Psi_{2j-1}\|^2 = \mathcal{N}^{-1}.$

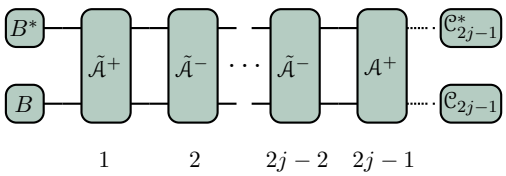

$\|\Psi_{2j}\|^2 = \mathcal{N}^{-1}.$

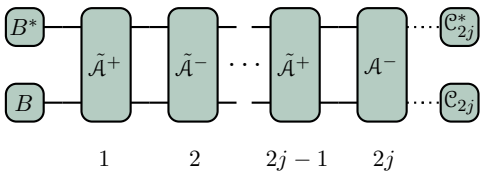

Here the various graphical elements are given by

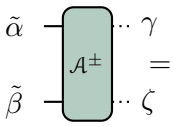

$$= \sum_{r=x,y,z} \left[(A^{\pm})^*\right]^r_{\tilde{\alpha},\gamma} \left[A^{\pm}\right]^r_{\tilde{\beta},\zeta} ,$$

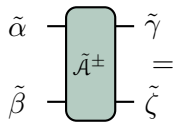

$$= \sum_{r=0,x,y,z} \left[(A^{\pm})^*\right]^r_{\tilde{\alpha},\tilde{\gamma}} \left[A^{\pm}\right]^r_{\tilde{\beta},\tilde{\zeta}} ,$$

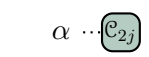

$$= B^{(R)}_{\alpha} \left([A^-]^0_{\alpha,\alpha}\right)^{\frac{N-2j}{2}} \left([A^+]^0_{\alpha,\alpha}\right)^{\frac{N-2j}{2}} .$$

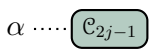

$$= B^{(R)}_{\alpha} \left([A^-]^0_{\alpha,\alpha}\right)^{\frac{N-2j}{2}} \left([A^+]^0_{\alpha,\alpha}\right)^{\frac{N-2j}{2}-1}$$

$$= B^{(L)}_{\tilde{\alpha}} .$$

Using the expressions for $A^{\pm}$ we find that

$$\tilde{\mathcal{A}}^+ = \tilde{\mathcal{A}}^- = \tilde{\mathcal{A}} , \tag{30}$$

which hugely simplifies the problem of calculating the norms. We diagonalize $\mathcal{A}$ by means of a similarity transformation S

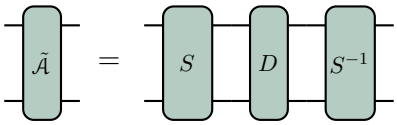

(31)

Explicit expressions for these matrices in given in appendix C. Using (31), we obtain

$$\|\Psi_{2j-1}\|^2 = \mathcal{N}^{-1} \cdot$$

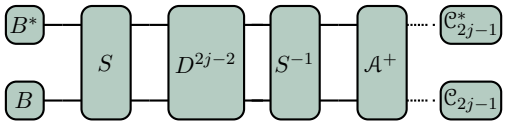

$$\|\Psi_{2j}\|^2 = \mathcal{N}^{-1} \cdot$$

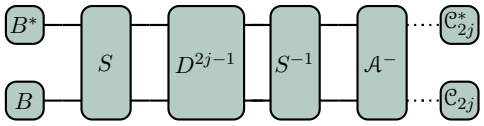

For large system sizes these expressions are dominated by the largest eigenvalue of D, which is smaller than 1 provided $\eta > 0$. The Hilbert-Schmidt norms therefore decay exponentially in j, yielding localization at the boundary for the ESZM. The asymptotic (in j) rate of exponential decay in the thermodynamic limit is given by

$$\lim_{N\to\infty} \|\Psi_j\|^2 \asymp a_1 \cdot (d_6)^{j-1} \qquad \text{for} \quad j \gg 1 , \tag{32}$$

where

$$\begin{aligned} d_6 =& \frac{\cos^2\left(\frac{\delta}{2}\right)\Big(2\cos\delta - \kappa + \cosh(2\eta)\,(\kappa+1) + 1\Big)}{\big(\cos\delta + \cosh(2\eta)\big)^2} < 1 \\ a_1 =& \frac{\sinh^2(\eta)\,\tanh^2(\eta)\Big(\kappa + 4(s^{(L)})^2(\cosh(2\eta)+1) - 1\Big)\Big(\sin^2\left(\frac{\delta}{2}\right)(\kappa+1) + 2\cosh^2(\eta)\Big)}{(4(s^{(L)})^2+1)\,\kappa\,\big(\cos\delta + \cosh(2\eta)\big)^2} , \\ \kappa =& \sqrt{5 + 4\cosh(2\eta)} . \end{aligned} \tag{33}$$

In Fig. 4 we show a comparison of the Hilbert-Schmidt norms of Ψ_j for a system of $N = 30$ sites with the asymptotic result (32) for a particular choice of boundary conditions. We

observe that the agreement is excellent. Further, we can quantify how well a truncation of the ESZM operator to the first j terms approximates the full operator. To that end we define

$$\Psi_{\leq j} = \sum_{n=1}^{j} \Psi_n \ , \tag{34}$$

and then evaluate the relative difference of the square of the norms

$$1 - \frac{\|\Psi_{\leq j}\|^2}{\|\Psi\|^2} \ . \tag{35}$$

As shown in Fig. 4) this quantity shows an exponential decay in j.

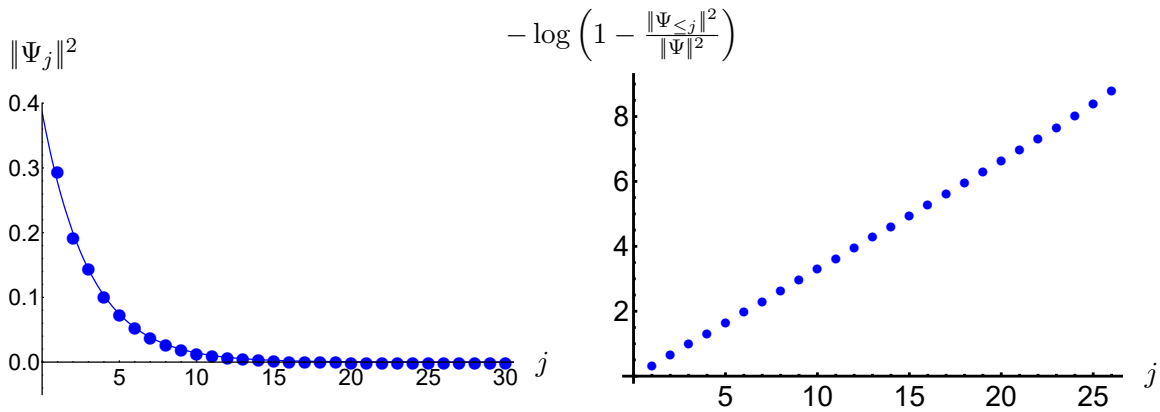

Figure 4: Left: Hilbert-Schmidt Norm of Ψ_j for $N = 30$, $\eta = 1.25$ and $\delta = 0.3$ while the boundary parameters are set to be $\xi^{(R)} = 0.28$, $s^{(R)} = 0.32$, $s^{(L)} = 0.45$, $\varphi^{(R)} = 0.67$, $\varphi^{(L)} = 0.97$. Blue dots are the numerical computed data points while the blue line is the predicted asymptotic behaviour (32). Right: negative logarithm of residual probability. One can see clearly a linear growth.

3 The spin-1/2 Heisenberg XXZ model

A local Hamiltonian $\mathbb{H}$ can be obtain by the first derivative of the transfer matrix at the shift point $u = 0$ if we set $\delta = 0$:

$$\frac{\mathrm{d}}{\mathrm{d}u}\bigg|_{u=0} \mathbb{T}(u,0) = 2\coth((\eta)\sinh(\xi^{(L)})\sinh(\xi^{(R)})\Big(\mathbb{H} - N\cosh(\eta) + \sinh(\eta)\tanh(\eta)\Big) \ . \tag{36}$$

Using this normalisation, we get the standard XXZ Hamiltonian subjected to boundary magnetic field:

$$\mathbb{H}_{\mathrm{XXZ}} = \sum_{j=1}^{N-1} \sigma_j^x\sigma_{j+1}^x + \sigma_j^y\sigma_{j+1}^y + \Delta\sigma_j^z\sigma_{j+1}^z + h_1 + h_N \ , \qquad \Delta = \cosh(\eta) \ . \tag{37}$$

The boundary terms are given explicitly by

$$\begin{aligned} h_1 &= -2\mathrm{i}s^{(L)}\sinh(\eta)\left(\mathrm{e}^{\mathrm{i}\varphi^{(L)}}\sigma_1^+ - \mathrm{e}^{-\mathrm{i}\varphi^{(L)}}\sigma_1^-\right) \ , \\ h_N &= \sinh(\eta)\coth(\xi^{(R)})\sigma_N^z + \frac{2s^{(R)}\sinh(\eta)}{\sinh(\xi^{(R)})}\left(\mathrm{e}^{\mathrm{i}\varphi^{(R)}}\sigma_N^+ + \mathrm{e}^{-\mathrm{i}\varphi^{(R)}}\sigma_N^-\right) \ . \end{aligned} \tag{38}$$

The Hamiltonian is Hermitian, since we take $s^{(L,R)}$, $\xi^{(R)} \in \mathbb{R}$ and $\varphi^{(L,R)} \in [0, 2\pi]$. All the results discussed in the previous section carry over in complete analogy, including the existence of the SZM and its localization properties, which can be obtained by taking the limit $\delta \to 0$ of the above equations. This limit is well behaved, ensuring that no singularities arise and that the structure of the conserved operators remains intact. Hence, we can consistently set

$$\lim_{\delta \to 0} \Psi = \Psi^{\mathrm{XXZ}} , \tag{39}$$

3.1 Infinite edge coherence times

A useful diagnostic for the presence of a strong zero mode are infinite temperature autocorrelation functions

$$C_0^{\mathcal{O}}(t) = \frac{1}{2^N} \mathrm{Tr}\left[\mathcal{O}(t)\mathcal{O}(0)\right] , \tag{40}$$

where $\mathcal{O}(0)$ are local operators that act non-trivially only very close to the left boundary. In generic spin chains such correlation functions decay in time to asymptotic values that go to zero as the system size increases. To see how an SZM operator Ψ localized around the left boundary affects $C^{\mathcal{O}}(t)$ from (40), we decompose $\mathcal{O}(0)$ as

$$\mathcal{O}(0) = c_1^{\mathcal{O}} \Psi + c_2^{\mathcal{O}} \mathcal{O}' , \qquad \mathrm{Tr}\big(\Psi^\dagger \mathcal{O}'\big) = 0 , \qquad c_1^{\mathcal{O}} \neq 0 , \tag{41}$$

where $c_1^{\mathcal{O}} = \mathcal{O}(L^0)$ for large system sizes and $\mathcal{O}'$ is by construction localized around the left boundary. Recalling that the ESZM is normalized $\|\Psi\|^2 = (2)^{-N} \mathrm{Tr}\left[\Psi^\dagger \Psi\right] = 1$ then gives

$$C_0^{\mathcal{O}}(t) = |c_1^{\mathcal{O}}|^2 + |c_2^{\mathcal{O}}|^2 C_0^{\mathcal{O}'}(t) . \tag{42}$$

The autocorrelator $C^{\mathcal{O}'}(t)$ is expected to decay in time to a value that vanishes as $N \to \infty$, which in turn implies that $C^{\mathcal{O}}(t)$ decays to a finite value $|c_1^{\mathcal{O}}|^2$ set by the overlap of $\mathcal{O}(0)$ with Ψ. In particular, we have

$$c_1^{\mathcal{O}} = \frac{1}{2^N} \mathrm{Tr}(\Psi^\dagger \mathcal{O}) . \tag{43}$$

The first few operators that are ultra-localized at the boundaries and have non-vanishing overlap with the ESZM operatopr are

$$\sigma_1^z , \qquad \sigma_1^x \sigma_2^z , \qquad \sigma_1^y \sigma_2^z . \tag{44}$$

The asymptotic values of the infinite temperature autocorrelation function of these in the limit $N \to \infty$ can be read off from (27)

$$\begin{aligned} |c_1^{\sigma_1^z}|^2 =& |c_{\Psi_1}|^2 \\ |c_1^{\sigma_1^x \sigma_2^z}|^2 =& |c_{\Psi_2} s^{(L)} \sinh(2\eta) \sin(\varphi^{(L)})|^2 \\ |c_1^{\sigma_1^y \sigma_2^z}|^2 =& |c_{\Psi_2} s^{(L)} \sinh(2\eta) \cos(\varphi^{(L)})|^2 . \end{aligned} \tag{45}$$

Here $c_{\Psi_{1,2}}$ are given by the $\delta \to 0$ limit of (28). The edge autocorrelation function $C_0^{\sigma_1^z}(t)$ is shown for $\delta = 2.5$, $N = 6, 8, 10$ and boundary fields $h_1 = (1, 0.1, 0)$, $h_N = (0.25, 0.5, 1)$ in Fig. 5. We observe that $C_0^{\sigma_1^z}(t)$ does not decay to zero but approaches a finite value at late times. The limiting value is in good agreement with the one predicted by the argument presented in eqn (42) and (45).

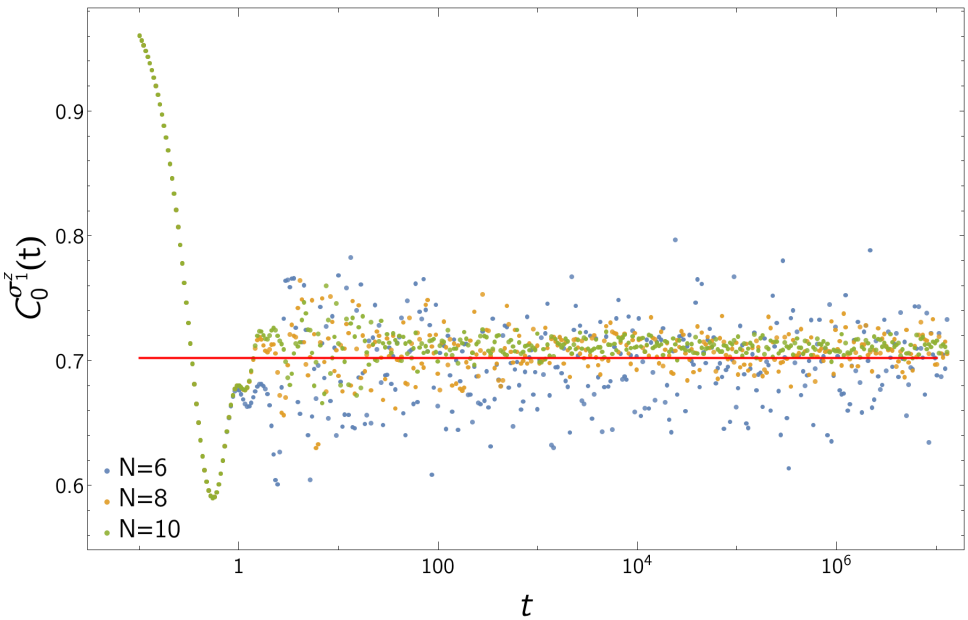

Figure 5: Infinite temperature autocorrelation function for $\Delta = 2.5$ and $h_1 = (1, 0.1, 0)$, $h_N = (0.25, 0.5, 1)$. The red line is $|c_{\Psi_1}|^2$ in the thermodynamic limit.

4 The asymmetric exclusion process

There is a well-known relation between the spin-1/2 XXZ chain and the asymmetric simple exclusion process (ASEP) [50–54]. The ASEP describes the biased diffusion of hard-core particles on a one-dimensional chain and is one of the best-studied paradigms of non-equilibrium Statistical Mechanics [55–57]. Of particular interest have been the effects of particle injection and extraction at the boundaries [54, 58–71], which can lead to boundary-induced phase transitions [72, 73].

The ASEP is a stochastic process on a one-dimensional lattice with N sites. At any given time t each site is either occupied by a particle or empty, and the system evolves subject to the following rules. On sites 2 to $N-1$ a particle attempts to hop one site to the right with rate p and one site to the left with rate $q = 1 - p$. The hop is executed unless the neighbouring site is occupied, in which case the move is rejected. On the first and last sites of the lattice these rules are modified by allowing particles to enter (leave) with rates α (γ) at site $i = 1$ and with rates δ (β) at site $i = N$ respectively, see Figure 6. The

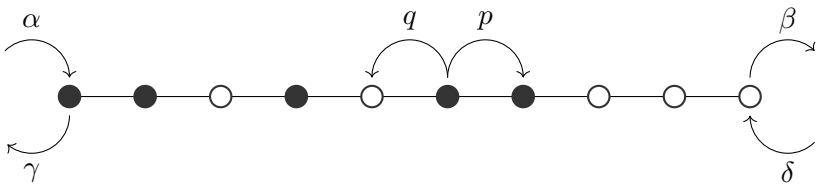

Figure 6: Dynamic rules for the ASEP with open boundary conditions.

master equation corresponding to these dynamical rules is obtained by associating a set $\boldsymbol{\tau} = \{\tau_1, \ldots, \tau_N\}$ of Boolean variables with the N sites of the lattice, indicating whether a particle is present at site i ($\tau_i = 1$) or not ($\tau_i = 0$). The state of the system at time t is then characterized by the probability distribution $P_t(\tau_1, \ldots, \tau_N)$. It is convenient to

associate a state in a linear vector space with $P_t(\boldsymbol{\tau})$ by defining [52]

$$|P_t\rangle = \sum_{\boldsymbol{\tau}} P_t(\boldsymbol{\tau})|\boldsymbol{\tau}\rangle \ ,$$
$$|\boldsymbol{\tau}\rangle = |\tau_1\rangle \otimes |\tau_2\rangle \otimes \cdots \otimes |\tau_L\rangle \ , \qquad |1\rangle = \begin{pmatrix}1\\0\end{pmatrix} \ , \qquad |0\rangle = \begin{pmatrix}0\\1\end{pmatrix} \tag{46}$$

The master equation then takes the form of an imaginary time Schrödinger equation with a non-Hermitian Hamiltonian

$$\frac{\partial|P\rangle}{\partial t} = \mathbb{H}|P\rangle \tag{47}$$

where the Hamiltonian $\mathbb{H}$ is given by

$$\mathbb{H} = \sum_{k=1}^{N-1}\Big[p\sigma_k^-\sigma_{k+1}^+ + q\sigma_k^+\sigma_{k+1}^- + \frac{p+q}{4}(\sigma_j^z\sigma_{j+1}^z - \mathbb{1}) + \frac{p-q}{4}(\sigma_{k+1}^z - \sigma_k^z)\Big] - B_1 - B_N. \tag{48}$$

Here the boundary terms take the form

$$B_1 = \frac{\alpha-\gamma}{2}\,\sigma_1^z - \alpha\sigma_1^- - \gamma\sigma_1^+ + \frac{\alpha+\gamma}{2} \ , \tag{49}$$
$$B_N = \frac{\delta-\beta}{2}\,\sigma_N^z - \delta\sigma_N^- - \beta\sigma_N^+ + \frac{\beta+\delta}{2} \ . \tag{50}$$

Performing a similarity transformation induced by the matrix

$$\mathcal{S} = \prod_{j=1}^{N}\begin{pmatrix}1 & 0\\ 0 & \Lambda Q^{j-1}\end{pmatrix}_j \tag{51}$$

where $Q = \sqrt{q/p}$ and Λ is a free parameter, we obtain the spin-1/2 XXZ chain Hamiltonian (37)

$$\mathcal{S}\mathbb{H}\mathcal{S}^{-1} = \frac{\sqrt{pq}}{2}\big(\mathbb{H}_{\rm XXZ} + (N-1)\cosh\eta\big) \ , \tag{52}$$

where the parameters are related by [54]

$$\cosh\eta = \frac{p+q}{2\sqrt{pq}} \ ,$$
$$h_1 = \Big(-\frac{\alpha-\gamma}{\sqrt{pq}} + \frac{q-p}{2\sqrt{pq}}\Big)\sigma_1^z + \frac{2\Lambda\alpha}{\sqrt{pq}}\sigma_1^- + \frac{2\gamma}{\Lambda\sqrt{pq}}\sigma_1^+ - \frac{\alpha+\gamma}{\sqrt{pq}} \ ,$$
$$h_N = \Big(-\frac{\delta-\beta}{\sqrt{pq}} - \frac{q-p}{2\sqrt{pq}}\Big)\sigma_N^z + \frac{2\Lambda\delta Q^{N-1}}{\sqrt{pq}}\sigma_N^- + \frac{2\beta Q^{1-N}}{\Lambda\sqrt{pq}}\sigma_N^+ - \frac{\beta+\delta}{\sqrt{pq}} \tag{53}$$

The above mapping implies that the transition matrix of the ASEP commutes with the operator

$$\mathbb{\Psi}^{\rm ASEP} = \mathcal{N}^{\rm ASEP}\mathcal{S}^{-1}\mathbb{\Psi}^{\rm XXZ}\mathcal{S} \ , \qquad [\mathbb{H}, \mathbb{\Psi}^{\rm ASEP}] = 0 \ , \tag{54}$$

where $\mathcal{N}^{\rm ASEP}$ is a normalization factor

$$\mathcal{N}^{\rm ASEP} = \Big[\prod_{j=2}^{N} g_j\Big]^{-\frac{1}{2}} \tag{55}$$

that ensures

$$0 < \lim_{N\to\infty} \frac{1}{2^N} \mathrm{Tr}\Big(\big(\mathbb{\Psi}^{\mathrm{ASEP}}\big)^\dagger \mathbb{\Psi}^{\mathrm{ASEP}} \Big) < \infty \,. \tag{56}$$

The normalisation factor we need to choose is dependent on the regime of η. For $\eta > \log(2+\sqrt{3})$ we have

$$g_j = \cosh\big((j-1)\eta + 2\log(\Lambda)\big)\,,$$

while for $\eta < \log(2+\sqrt{3})$ we need to choose

$$\begin{aligned} g_j = &\cosh\big((j-1)\eta + 2\log(\Lambda)\big)\frac{1}{16}\Bigg(8\mathrm{sech}^3(\eta)(\cosh(\eta)+\cosh(2\eta)+\mathrm{sech}(\eta)-1) \\ &+ \sinh^2(2\eta)\sqrt{10\cosh(\eta)+4\cosh(2\eta)+2}\mathrm{csch}\left(\frac{\eta}{2}\right)\mathrm{sech}^6(\eta)\Bigg)\,. \end{aligned}$$

In order to ascertain whether the operator $\mathbb{\Psi}^{\mathrm{ASEP}}$ is still localized around the left boundary we need to determine its spatial locality structure. The composition of the ESZM in the XXZ chain

$$\mathbb{\Psi}^{\mathrm{XXZ}} = \sum_{j=0}^{N} \Psi_j^{\mathrm{XXZ}} \tag{57}$$

is inherited by the ESZM in the ASEP

$$\mathbb{\Psi}^{\mathrm{ASEP}} = \mathcal{N}^{\mathrm{ASEP}} \sum_{j=0}^{N} \mathcal{S}^{-1}\Psi_j^{\mathrm{XXZ}}\mathcal{S} = \sum_{j=0}^{N} \Psi_j^{\mathrm{ASEP}}. \tag{58}$$

In order to ascertain whether the Ψ_j^{ASEP} have good spatial locality structures we calculate their Hilbert-Schmidt norms. Using that $\mathcal{S} = \mathcal{S}^\dagger$ we have

$$\|\Psi_j^{\mathrm{ASEP}}\|^2 = \frac{\big(\mathcal{N}^{\mathrm{ASEP}}\big)^2}{2^N} \cdot \mathrm{Tr}\Bigg(\big(\mathcal{S}(\Psi_j^{\mathrm{XXZ}})^\dagger \mathcal{S}^{-1}\mathcal{S}^{-1}\Psi_j^{\mathrm{XXZ}}\mathcal{S}\big) \Bigg)\,.$$

This is conveniently evaluated using a MPO representation

$\|\Psi_j^{\mathrm{ASEP}}\|^2 = \mathcal{N}^{-1}.$

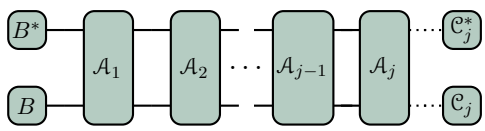

Here the various elements are given by

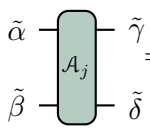

$$= \sum_{\rho_1,\rho_2=0,x,y} \big[A^*\big]^{\rho_1}_{\tilde{\alpha},\tilde{\gamma}} \big[A\big]^{\rho_2}_{\tilde{\beta},\tilde{\delta}} \cdot (g_j)^{-1}\mathrm{Tr}\big(\mathcal{S}_j\sigma^{\rho_1}(\mathcal{S}_j\mathcal{S}_j)^{-1}\sigma^{\rho_2}\mathcal{S}_j\big)$$

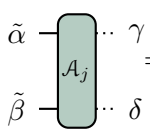

$$= \sum_{\rho_1,\rho_2=x,y,z} \big[A^{\rho_1}_{\tilde{\alpha},\gamma}\big]^* \big[A^{\rho_2}_{\tilde{\beta},\delta}\big] \cdot (g_j)^{-1}\mathrm{Tr}\big(\mathcal{S}_j\sigma^{\rho_1}(\mathcal{S}_j\mathcal{S}_j)^{-1}\sigma^{\rho_2}\mathcal{S}_j\big)$$

$\tilde{\alpha} = B^{(L)}_{\tilde{\alpha}}$

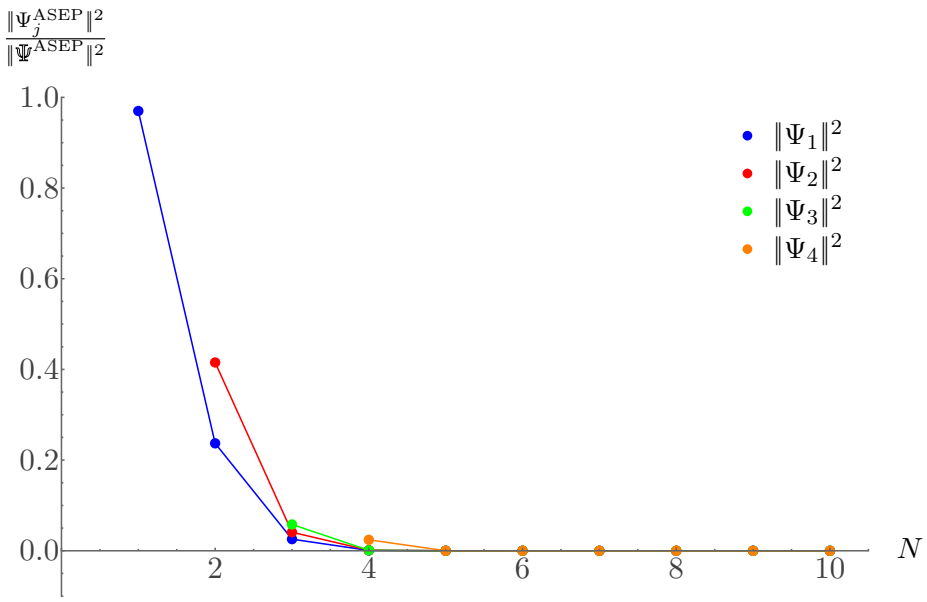

Figure 7: Normalized Hilbert Schmidt norms of $\Psi_j^{\rm ASEP}$ for $j = 1, 2, 3, 4$ as functions of the system size N. We observe that the contribution of $\Psi_j^{\rm ASEP}$ becomes negligible as N increases at fixed j, implying that that (58) is not localised in the vicinity of the boundary. The system parameters are $s^{(R)} = 0.13$, $s^{(L)} = 0.7$, $\varphi^{(L)} = 0.68$, $\varphi^{(R)} = 0.98$, $\xi^{(R)} = 0.25$, $\eta = 1.35$ and $\Lambda = 1.1$.

$\alpha \cdots \boxed{\mathcal{C}_j} \quad = \prod_{k=j+1}^{N} (g_j)^{-\frac{1}{2}} \left([A]^0_{\alpha,\alpha}\right)^{N-j} B^{(R)}_\alpha$

and we use the homogeneous limit of the MPO matrices introduced earlier

$$A \equiv \lim_{\delta \to 0} A^{\pm} \ . \tag{59}$$

We find that $\|\Psi_j^{\rm ASEP}\|^2 \to 0$ as $N \to \infty$ for any j including $j = 1$, yielding no localization at the boundary! This behaviour originates from the exponentially suppressing factor in the $\mathcal{C}_j$ matrix when $N \to \infty$, which was absent for the quantum circuit/XXZ case but needed in the ASEP to ensure (56). Numerical data is represented in Figure 7.

5 Conclusions

In this work, we have constructed exact strong zero mode operators for both integrable quantum brick-wall circuits and the spin-1/2 Heisenberg XXZ spin chain with the most general integrable boundary conditions compatible with respectively unitarity and Hermiticity. This generalizes previous studies in the literature [5, 20] in that the boundary conditions break the $U(1)$ symmetry present in the bulk of the system, and magnetization is therefore no longer conserved under time evolution. We have derived an explicit matrix product operator (MPO) form for the ESZM operators and used this representation to prove that they are localized (by construction) around the left boundary of the system.

The presence of an ESZM is expected to give rise to infinite coherence time for autocorrelation functions of certain operators localized near the boundary. We have verified numerically that this is indeed the case for σ_1^z autocorrelation functions the XXZ model,

and have observed that the asymptotic value reached at late time agrees with considerations based on the finite overlap of σ_1^z with the ESZM operator.

There is a well-known map between the spin-1/2 Heisenberg XXZ chain with open boundary conditions and the asymmetric exclusion process and the existence of an ESZM operator in the former poses the question of what role, if any, this plays in the latter. We have shown that under the map the ESZM loses its defining property of being spatially localized in the vicinity of the boundaries. This implies that it cannot affect the local properties of the ASEP in a significant way.

The effects of the presence of strong zero modes in kicked Ising models has been previously investigated in systems of transmon qubits in [74]. The brick-wall quantum circuit studied here has been realized in the same device [37], and it would be interesting to investigate boundary effects in this system in light of our findings.

Acknowledgments

This work was supported by the EPSRC under grant EP/X030881/1. We are grateful to Eric Vernier and Paul Fendley for many helpful discussions.

A Explicit matrix elements of the SZM as MPO

To get the homogeneous limit set $\delta = 0$. The explicit non-vanishing matrix elements are given by

$$\begin{aligned}
\left[A^{\pm}\right]^0_{0,0} &= \cos^2\left(\tfrac{\delta}{2}\right)\mathrm{sech}\left(\tfrac{\mathrm{i}\delta}{2}-\eta\right)\mathrm{sech}\left(\tfrac{\mathrm{i}\delta}{2}+\eta\right)\ ,\\
\left[A^{\pm}\right]^0_{x,x} &= \cos^2\left(\tfrac{\delta}{2}\right)\cosh(\eta)\mathrm{sech}\left(\tfrac{\mathrm{i}\delta}{2}-\eta\right)\mathrm{sech}\left(\tfrac{\mathrm{i}\delta}{2}+\eta\right)\ ,\\
\left[A^{\pm}\right]^0_{y,y} &= \cos^2\left(\tfrac{\delta}{2}\right)\cosh(\eta)\mathrm{sech}\left(\tfrac{\mathrm{i}\delta}{2}-\eta\right)\mathrm{sech}\left(\tfrac{\mathrm{i}\delta}{2}+\eta\right)\ ,\\
\left[A^{\pm}\right]^0_{z,z} &= 1\,,
\end{aligned} \tag{60}$$

$$\begin{aligned}
\left[A^{\pm}\right]^x_{0,x} &= +\left[A^{\pm}\right]^y_{0,y} = \mathrm{i}\cos\left(\tfrac{\delta}{2}\right)\sinh(\eta)\mathrm{sech}\left(\tfrac{\mathrm{i}\delta}{2}-\eta\right)\mathrm{sech}\left(\tfrac{\mathrm{i}\delta}{2}+\eta\right)\ ,\\
\left[A^{\pm}\right]^x_{x,0} &= +\left[A^{\pm}\right]^y_{y,0} = \mathrm{i}\cos\left(\tfrac{\delta}{2}\right)\sinh(\eta)\cosh(\eta)\mathrm{sech}\left(\tfrac{\mathrm{i}\delta}{2}-\eta\right)\mathrm{sech}\left(\tfrac{\mathrm{i}\delta}{2}+\eta\right)\ ,\\
\left[A^{\pm}\right]^x_{y,z} &= -\left[A^{\pm}\right]^y_{x,z} = \mp\mathrm{i}\sin\left(\tfrac{\delta}{2}\right)\sinh^2(\eta)\mathrm{sech}\left(\tfrac{\mathrm{i}\delta}{2}-\eta\right)\mathrm{sech}\left(\tfrac{\mathrm{i}\delta}{2}+\eta\right)\ ,
\end{aligned} \tag{61}$$

$$\begin{aligned}
\left[A^{\pm}\right]^z_{0,z} &= \sinh^2(\eta)\mathrm{sech}\left(\tfrac{\mathrm{i}\delta}{2}-\eta\right)\mathrm{sech}\left(\tfrac{\mathrm{i}\delta}{2}+\eta\right)\ ,\\
\left[A^{\pm}\right]^z_{x,y} &= \pm\tfrac{1}{2}\sin(\delta)\sinh(\eta)\mathrm{sech}\left(\tfrac{\mathrm{i}\delta}{2}-\eta\right)\mathrm{sech}\left(\tfrac{\mathrm{i}\delta}{2}+\eta\right)\ ,\\
\left[A^{\pm}\right]^z_{y,x} &= \mp\tfrac{1}{2}\sin(\delta)\sinh(\eta)\mathrm{sech}\left(\tfrac{\mathrm{i}\delta}{2}-\eta\right)\mathrm{sech}\left(\tfrac{\mathrm{i}\delta}{2}+\eta\right)\ ,
\end{aligned} \tag{62}$$

$$\begin{aligned}
B_0^{(L)} &= 1\ ,\\
B_x^{(L)} &= -2\mathrm{i}s^{(L)}\sin(\varphi^{(L)})\ ,\\
B_y^{(L)} &= +2\mathrm{i}s^{(L)}\cos(\varphi^{(L)})\ ,
\end{aligned} \tag{63}$$

$$
\begin{aligned}
B_0^{(R)} &= -\,2\mathrm{i}\sinh(\eta)\sinh(\xi^{(R)})\ ,\\
B_x^{(R)} &= -\,2s^{(R)}\cos(\varphi^{(R)})\sinh(2\eta)\ ,\\
B_y^{(R)} &= -\,2s^{(R)}\sin(\varphi^{(R)})\sinh(2\eta)\ ,\\
B_z^{(R)} &= -\,2\mathrm{i}\cosh(\xi^{(R)})\cosh(\eta)\ .
\end{aligned}
\tag{64}
$$

B Normalisation Constant for Finite system sizes

For completeness sake we here report the normalization constant on the ESZM in a finite volume N

$$
\begin{aligned}
\mathcal{N} =& \frac{2}{\kappa}\Bigg(\sinh^2(2\eta)\Big[-4\kappa\big(s^{(L)}\big)^2\lambda_4^L\big(s^{(R)}\big)^2\cos\big(2(\phi^{(L)}-\phi^{(R)})\big)\\
&+2\kappa\big(s^{(L)}\big)^2\big(s^{(R)}\big)^2(\lambda_6^L+\lambda_7^L)-(\lambda_6^L-\lambda_7^L)\Big(\big(s^{(L)}\big)^2\cosh\big(2\xi^{(R)}\big)\\
&+2\Big(\big(s^{(L)}\big)^2+1\Big)\big(s^{(R)}\big)^2-\big(s^{(L)}\big)^2\Big)\Big]\\
&-16\sinh^2(\eta)\cosh(\eta)\kappa s^{(L)}s^{(R)}\lambda_5^L\sinh\big(\xi^{(R)}\big)\sin\big(\phi^{(L)}-\phi^{(R)}\big)\\
&-\cosh^2(\eta)\cosh^2\big(\xi^{(R)}\big)\Big[-4\cosh(2\eta)\big(s^{(L)}\big)^2\Big(\lambda_6^L-\lambda_7^L\Big)\\
&+\kappa\Big(4\big(s^{(L)}\big)^2\Big(-2\lambda_3^L+\lambda_6^L+\lambda_7^L\Big)+\lambda_6^L+\lambda_7^L\Big)-\Big(8\big(s^{(L)}\big)^2+3\Big)\Big(\lambda_6^L-\lambda_7^L\Big)-2\kappa\lambda_3^L\Big]\\
&+\sinh^2(\eta)\sinh^2\big(\xi^{(R)}\big)\Big(\Big(\kappa+1\Big)\lambda_6^L+\Big(\kappa-1\Big)\lambda_7^L\Big)\Bigg),
\end{aligned}
$$

where we recall $N=2L$ and we have further

$$
\begin{aligned}
\kappa =& \sqrt{4\cosh(2\eta)+5}\\
\lambda_1 =& \frac{(\cos\delta+1)^2}{\big(\cos\delta+\cosh(2\eta)\big)^2},\\
\lambda_2 =& \frac{4\cos^4\!\big(\frac{\delta}{2}\big)\,\cosh^2\eta}{\big(\cos\delta+\cosh(2\eta)\big)^2},\\
\lambda_3 =& 1,\\
\lambda_4 =& \frac{4\cos^4\!\big(\frac{\delta}{2}\big)\,\big(\cos\delta\,\cosh(2\eta)+1\big)^2}{\big(\cos\delta+\cosh(2\eta)\big)^4},\\
\lambda_5 =& \frac{4\cos^4\!\big(\frac{\delta}{2}\big)\,\cosh^2\eta\,\big(\cos\delta-\cosh(2\eta)+2\big)^2}{\big(\cos\delta+\cosh(2\eta)\big)^4},\\
\lambda_6 =& \frac{\cos^4\!\big(\frac{\delta}{2}\big)}{\kappa\,\big(\cos\delta+\cosh(2\eta)\big)^4}\Big[-20\,(2\cos\delta+1)\,\sinh^2\eta+8\cos\delta\,\kappa\,\cosh^2\eta+(2\cos(2\delta)+7)\,\kappa\\
&-\cosh(2\eta)\Big(4\sinh^2\eta\,\big(8\cos\delta+4\cosh(2\eta)+9\big)+\kappa\Big)+\big(\cosh(6\eta)-\cosh(4\eta)\big)\,\kappa\Big],\\
\lambda_7 =& \frac{\cos^4\!\big(\frac{\delta}{2}\big)}{\kappa\,\big(\cos\delta+\cosh(2\eta)\big)^4}\Big[\,20\,(2\cos\delta+1)\,\sinh^2\eta+8\cos\delta\,\kappa\,\cosh^2\eta+(2\cos(2\delta)+7)\,\kappa\\
&+\cosh(2\eta)\Big(4\sinh^2\eta\,\big(8\cos\delta+4\cosh(2\eta)+9\big)-\kappa\Big)+\big(\cosh(6\eta)-\cosh(4\eta)\big)\,\kappa\Big].
\end{aligned}
$$

All the eigenvalues λ_j are smaller than one expect $\lambda_3 \equiv 1$, which the dominant term as $N \to \infty$.

C Diagonalisation of $\tilde{\mathcal{A}}$

We have

$$\tilde{\mathcal{A}} = SDS^{-1} \tag{65}$$

$$\begin{aligned}
D &= \operatorname{diag}\{d_1, d_2, d_2, d_3, d_3, d_4, d_4, d_5, d_6\} \\
d_1 &= \frac{\cos\delta + 1}{\cos\delta + \cosh(2\eta)}, \\
d_2 &= \frac{2\cos^2\left(\frac{\delta}{2}\right)\left(\cos\delta\,\cosh(2\eta) + 1\right)}{\left(\cos\delta + \cosh(2\eta)\right)^2}, \\
d_3 &= \frac{2\cos^2\left(\frac{\delta}{2}\right)\cosh\eta\left(\cos\delta - \cosh(2\eta) + 2\right)}{\left(\cos\delta + \cosh(2\eta)\right)^2}, \\
d_4 &= \frac{\left(\cos\delta + 1\right)\cosh\eta}{\cos\delta + \cosh(2\eta)}, \\
d_5 &= \frac{\cos^2\left(\frac{\delta}{2}\right)\Big(2\cos\delta - \cosh(2\eta)\,(\kappa - 1) + \kappa + 1\Big)}{\left(\cos\delta + \cosh(2\eta)\right)^2}, \\
d_6 &= \frac{\cos^2\left(\frac{\delta}{2}\right)\Big(2\cos\delta - \kappa + \cosh(2\eta)\,(\kappa + 1) + 1\Big)}{\left(\cos\delta + \cosh(2\eta)\right)^2}.
\end{aligned} \tag{66}$$

$$S = \begin{pmatrix}
0 & 0 & 0 & 0 & 0 & 0 & 0 & -\frac{1}{2}(\kappa+1)\operatorname{sech}^2(\eta) & \frac{1}{2}(\kappa-1)\operatorname{sech}^2(\eta) \\
0 & 0 & 0 & 0 & -1 & 0 & 1 & 0 & 0 \\
0 & 0 & 0 & -1 & 0 & 1 & 0 & 0 & 0 \\
0 & 0 & 0 & 0 & 1 & 0 & 1 & 0 & 0 \\
0 & -1 & 0 & 0 & 0 & 0 & 0 & 1 & 1 \\
-1 & 0 & 1 & 0 & 0 & 0 & 0 & 0 & 0 \\
0 & 0 & 0 & 1 & 0 & 1 & 0 & 0 & 0 \\
1 & 0 & 1 & 0 & 0 & 0 & 0 & 0 & 0 \\
0 & 1 & 0 & 0 & 0 & 0 & 0 & 1 & 1
\end{pmatrix} \tag{67}$$

References

[1] Z.-C. Gu and X.-G. Wen, *Tensor-entanglement-filtering renormalization approach and symmetry-protected topological order*, Physical Review B **80**(15) (2009), doi:10.1103/physrevb.80.155131.

[2] F. Pollmann, E. Berg, A. M. Turner and M. Oshikawa, *Symmetry protection of topological phases in one-dimensional quantum spin systems*, Physical Review B **85**(7) (2012), doi:10.1103/physrevb.85.075125.

[3] A. Y. Kitaev, *Unpaired majorana fermions in quantum wires*, Physics-uspekhi **44**(10S), 131 (2001), doi:10.1070/1063-7869/44/10S/S29.

[4] P. Fendley, *Parafermionic edge zero modes in Z_n-invariant spin chains*, Journal of Statistical Mechanics: Theory and Experiment **2012**(11), P11020 (2012), doi:10.1088/1742-5468/2012/11/P11020.

[5] P. Fendley, *Strong zero modes and eigenstate phase transitions in the XYZ/interacting majorana chain*, Journal of Physics A: Mathematical and Theoretical **49**(30), 30LT01 (2016), doi:/10.1088/1751-8113/49/30/30LT01.

[6] N. Moran, D. Pellegrino, J. K. Slingerland and G. Kells, *Parafermionic clock models and quantum resonance*, Phys. Rev. B **95**(23), 235127 (2017), doi:10.1103/PhysRevB.95.235127.

[7] L. M. Vasiloiu, F. Carollo, M. Marcuzzi and J. P. Garrahan, *Strong zero modes in a class of generalized Ising spin ladders with plaquette interactions*, Phys. Rev. B **100**(2), 024309 (2019), doi:10.1103/PhysRevB.100.024309.

[8] J. Kemp, N. Y. Yao and C. R. Laumann, *Symmetry-enhanced boundary qubits at infinite temperature*, Physical Review Letters **125**(20), 200506 (2020), doi:10.1103/PhysRevLett.125.200506.

[9] J. Kemp, N. Y. Yao, C. R. Laumann and P. Fendley, *Long coherence times for edge spins*, Journal of Statistical Mechanics: Theory and Experiment **2017**(6), 063105 (2017), doi:/10.1088/1742-5468/aa73f0.

[10] D. V. Else, P. Fendley, J. Kemp and C. Nayak, *Prethermal strong zero modes and topological qubits*, Physical Review X **7**(4), 041062 (2017), doi:10.1103/PhysRevX.7.041062.

[11] M. Thakurathi, A. A. Patel, D. Sen and A. Dutta, *Floquet generation of majorana end modes and topological invariants*, Phys. Rev. B **88**, 155133 (2013), doi:10.1103/PhysRevB.88.155133.

[12] A. Chandran, V. Khemani, C. R. Laumann and S. L. Sondhi, *Many-body localization and symmetry-protected topological order*, Phys. Rev. B **89**, 144201 (2014), doi:10.1103/PhysRevB.89.144201.

[13] Y. Bahri, R. Ronen and E. Altman, *Localization and topology protected quantum coherence at the edge of hot matter*, Nature Communications **6**, 7341 (2015), doi:10.1038/ncomms8341.

[14] T. Iadecola, L. H. Santos and C. Chamon, *Stroboscopic symmetry-protected topological phases*, Phys. Rev. B **92**, 125107 (2015), doi:10.1103/PhysRevB.92.125107.

[15] V. Khemani, A. Lazarides, R. Moessner and S. L. Sondhi, *Phase structure of driven quantum systems*, Phys. Rev. Lett. **116**, 250401 (2016), doi:10.1103/PhysRevLett.116.250401.

[16] G. J. Sreejith, A. Lazarides and R. Moessner, *Parafermion chain with $2\pi/k$ floquet edge modes*, Phys. Rev. B **94**, 045127 (2016), doi:10.1103/PhysRevB.94.045127.

[17] I.-D. Potirniche, A. C. Potter, M. Schleier-Smith, A. Vishwanath and N. Y. Yao, *Floquet symmetry-protected topological phases in cold-atom systems*, Phys. Rev. Lett. **119**, 123601 (2017), doi:10.1103/PhysRevLett.119.123601.

[18] A. Kumar, P. T. Dumitrescu and A. C. Potter, *String order parameters for one-dimensional floquet symmetry protected topological phases*, Phys. Rev. B **97**, 224302 (2018), doi:10.1103/PhysRevB.97.224302.

[19] B. Mukherjee, R. Melendrez, M. Szyniszewski, H. J. Changlani and A. Pal, *Emergent strong zero mode through local floquet engineering*, Phys. Rev. B **109**, 064303 (2024), doi:/10.1103/PhysRevB.109.064303.

[20] E. Vernier, H.-C. Yeh, L. Piroli and A. Mitra, *Strong zero modes in integrable quantum circuits*, Phys. Rev. Lett. **133**, 050606 (2024), doi:10.1103/PhysRevLett.133.050606.

[21] K. Klobas, P. Fendley and J. P. Garrahan, *Stochastic strong zero modes and their dynamical manifestations*, Phys. Rev. E **107**(4), L042104 (2023), doi:10.1103/PhysRevE.107.L042104.

[22] C. T. Olund, N. Y. Yao and J. Kemp, *Boundary strong zero modes*, Phys. Rev. B **111**, L201114 (2025), doi:10.1103/PhysRevB.111.L201114.

[23] D. J. Yates, F. H. L. Essler and A. Mitra, *Almost strong* $(0, \pi)$ *edge modes in clean interacting one-dimensional floquet systems*, Phys. Rev. B **99**, 205419 (2019), doi:10.1103/PhysRevB.99.205419.

[24] D. J. Yates, A. G. Abanov and A. Mitra, *Lifetime of almost strong edge-mode operators in one-dimensional, interacting, symmetry protected topological phases*, Phys. Rev. Lett. **124**, 206803 (2020), doi:/10.1103/PhysRevLett.124.206803.

[25] J. Alicea and P. Fendley, *Topological phases with parafermions: theory and blueprints*, Ann. Rev. Condensed Matter Phys. **7**, 119 (2016), doi:10.1146/annurev-conmatphys-031115-011336, 1504.02476.

[26] F. H. L. Essler, P. Fendley and E. Vernier, *Strong zero modes in integrable spin-s chains with open boundaries*, *to appear* (2025).

[27] V. Gritsev and A. Polkovnikov, *Integrable Floquet dynamics*, SciPost Phys. **2**, 021 (2017), doi:10.21468/SciPostPhys.2.3.021.

[28] M. Vanicat, L. Zadnik and T. Prosen, *Integrable trotterization: Local conservation laws and boundary driving*, Phys. Rev. Lett. **121**, 030606 (2018), doi:10.1103/PhysRevLett.121.030606.

[29] M. Ljubotina, L. Zadnik and T. Prosen, *Ballistic spin transport in a periodically driven integrable quantum system*, Phys. Rev. Lett. **122**, 150605 (2019), doi:10.1103/PhysRevLett.122.150605.

[30] M. Medenjak, T. Prosen and L. Zadnik, *Rigorous bounds on dynamical response functions and time-translation symmetry breaking*, SciPost Phys. **9**, 003 (2020), doi:10.21468/SciPostPhys.9.1.003.

[31] Y. Miao and E. Vernier, *Integrable Quantum Circuits from the Star-Triangle Relation*, Quantum **7**, 1160 (2023), doi:10.22331/q-2023-11-03-1160.

[32] I. L. Aleiner, *Bethe ansatz solutions for certain periodic quantum circuits*, Annals of Physics **433**, 168593 (2021), doi:/10.1016/j.aop.2021.168593.

[33] P. W. Claeys, J. Herzog-Arbeitman and A. Lamacraft, *Correlations and commuting transfer matrices in integrable unitary circuits*, SciPost Phys. **12**, 007 (2022), doi:10.21468/SciPostPhys.12.1.007.

[34] E. Vernier, B. Bertini, G. Giudici and L. Piroli, *Integrable digital quantum simulation: Generalized gibbs ensembles and trotter transitions*, Phys. Rev. Lett. **130**, 260401 (2023), doi:10.1103/PhysRevLett.130.260401.

[35] M. Takahashi, *Correlation length and free energy of the $s = 1/2$ XYZ chain*, Physical Review B **43**(7), 5788 (1991), doi:10.1103/PhysRevB.43.5788.

[36] D. B. Abraham, F. H. L. Essler and F. T. Latrémolière, *Correlation functions in an exactly solvable tefface-ledge-kink model*, Nucl. Phys. B **556**, 411 (1999), doi:10.1016/S0550-3213(99)00268-0.

[37] A. Morvan, T. I. Andersen, X. Mi, C. Neill, A. Petukhov, K. Kechedzhi, D. Abanin, A. Michailidis, R. Acharya, F. Arute *et al.*, *Formation of robust bound states of interacting microwave photons*, Nature **612**(7939), 240 (2022), doi:10.1038/s41586-022-05348-y.

[38] N. Keenan, N. F. Robertson, T. Murphy, S. Zhuk and J. Goold, *Evidence of kardar-parisi-zhang scaling on a digital quantum simulator*, npj Quantum Information **9**(1), 72 (2023), doi:10.1038/s41534-023-00742-4.

[39] K. Maruyoshi, T. Okuda, J. W. Pedersen, R. Suzuki, M. Yamazaki and Y. Yoshida, *Conserved charges in the quantum simulation of integrable spin chains*, Journal of Physics A: Mathematical and Theoretical **56**(16), 165301 (2023), doi:10.1088/1751-8121/acc369.

[40] E. K. Sklyanin, *Boundary conditions for integrable quantum systems*, Journal of Physics A: Mathematical and General **21**(10), 2375 (1988), doi:10.1088/0305-4470/21/10/015.

[41] H. J. de Vega and González-Ruiz, *Boundary k-matrices for the XYZ, XXZ and XXX spin chains*, Journal of Physics A: Mathematical and General **27**(18), 6129 (1994), doi:10.1088/0305-4470/27/18/021.

[42] V. E. Korepin, N. M. Bogoliubov and A. G. Izergin, *Quantum Inverse Scattering Method and Correlation Functions*, Cambridge Monographs on Mathematical Physics. Cambridge University Press, doi:10.1017/cbo9780511628832 (1993).

[43] I. V. Cherednik, *Factorizing Particles on a Half Line and Root Systems*, Theor. Math. Phys. **61**, 977 (1984), doi:10.1007/BF01038545.

[44] L. D'Alessio and M. Rigol, *Long-time behavior of isolated periodically driven interacting lattice systems*, Physical Review X **4**(4), 041048 (2014), doi:10.1103/PhysRevX.4.041048.

[45] A. Lazarides, A. Das and R. Moessner, *Equilibrium states of generic quantum systems subject to periodic driving*, Physical Review E **90**(1), 012110 (2014), doi:10.1103/PhysRevE.90.012110.

[46] P. Ponte, A. Chandran, Z. Papić and D. A. Abanin, *Periodically driven ergodic and many-body localized quantum systems*, Annals of Physics **353**, 196 (2015), doi:10.1016/j.aop.2014.11.008.

[47] A. Lazarides, A. Das and R. Moessner, *Periodic thermodynamics of isolated quantum systems*, Physical review letters **112**(15), 150401 (2014), doi:/10.1103/PhysRevLett.112.150401.

[48] F. H. L. Essler and M. Fagotti, *Quench dynamics and relaxation in isolated integrable quantum spin chains*, Journal of Statistical Mechanics: Theory and Experiment **2016**(6), 064002 (2016), doi:10.1088/1742-5468/2016/06/064002.

[49] P. Fendley, S. Gehrmann, E. Vernier and F. Verstraete, *XYZ integrability the easy way* (2025), doi:/10.48550/arXiv.2511.04674.

[50] L.-H. Gwa and H. Spohn, *Six-vertex model, roughened surfaces, and an asymmetric spin hamiltonian*, Phys. Rev. Lett. **68**, 725 (1992), doi:10.1103/PhysRevLett.68.725.

[51] L.-H. Gwa and H. Spohn, *Bethe solution for the dynamical-scaling exponent of the noisy burgers equation*, Phys. Rev. A **46**, 844 (1992), doi:10.1103/PhysRevA.46.844.

[52] F. C. Alcaraz, M. Droz, M. Henkel and V. Rittenberg, *Reaction-diffusion processes, critical dynamics, and quantum chains*, Ann. Phys. (N. Y.) **230**(2), 250 (1994), doi:10.1006/aphy.1994.1026.

[53] S. Sandow, *Partially asymmetric exclusion process with open boundaries*, Phys. Rev. E **50**, 2660 (1994), doi:10.1103/PhysRevE.50.2660.

[54] F. H. L. Essler and V. Rittenberg, *Representations of the quadratic algebra and partially asymmetric diffusion with open boundaries*, Journal of Physics A: Mathematical and General **29**(13), 3375 (1996), doi:10.1088/0305-4470/29/13/013.

[55] B. Derrida, *An exactly soluble non-equilibrium system: the asymmetric simple exclusion process*, Phys. Rep. **301**(1-3), 65 (1998), doi:10.1016/S0370-1573(98)00006-4.

[56] G. M. Schütz, *Exactly solvable models for many-body systems far from equilibrium*, In *Phase transitions and critical phenomena*, vol. 19, pp. 1–251. Elsevier, doi:10.1016/S1062-7901(01)80015-X (2001).

[57] K. Mallick, *Some exact results for the exclusion process*, J. Stat. Mech. **2011**(01), P01024 (2011), doi:10.1088/1742-5468/2011/01/P01024.

[58] B. Derrida, M. R. Evans, V. Hakim and V. Pasquier, *Exact solution of a 1d asymmetric exclusion model using a matrix formulation*, J. Phys. A **26**(7), 1493 (1993), doi:10.1088/0305-4470/26/7/011.

[59] G. Schütz and E. Domany, *Phase transitions in an exactly soluble one-dimensional exclusion process*, Journal of statistical physics **72**(1), 277 (1993), doi:10.1007/BF01048050.

[60] T. Sasamoto, *One-dimensional partially asymmetric simple exclusion process with open boundaries: orthogonal polynomials approach*, Journal of Physics A: Mathematical and General **32**(41), 7109 (1999), doi:10.1088/0305-4470/32/41/306.

[61] T. Sasamoto, *Density profile of the one-dimensional partially asymmetric simple exclusion process with open boundaries*, Journal of the Physical Society of Japan **69**(4), 1055 (2000), doi:10.1143/JPSJ.69.1055.

[62] R. A. Blythe, M. R. Evans, F. Colaiori and F. H. L. Essler, *Exact solution of a partially asymmetric exclusion model using a deformed oscillator algebra*, Journal of Physics A: Mathematical and General **33**(12), 2313 (2000), doi:10.1088/0305-4470/33/12/301.

[63] M. Uchiyama, T. Sasamoto and M. Wadati, *Asymmetric simple exclusion process with open boundaries and askey–wilson polynomials*, Journal of Physics A: Mathematical and General **37**(18), 4985 (2004), doi:10.1088/0305-4470/37/18/006.

[64] C. Enaud and B. Derrida, *Large deviation functional of the weakly asymmetric exclusion process*, Journal of statistical physics **114**(3), 537 (2004), doi:10.1023/B:JOSS.0000012501.43746.cf.

[65] J. de Gier and F. H. L. Essler, *Bethe ansatz solution of the asymmetric exclusion process with open boundaries*, Phys. Rev. Lett. **95**, 240601 (2005), doi:10.1103/PhysRevLett.95.240601.

[66] J. de Gier and F. H. L. Essler, *Exact spectral gaps of the asymmetric exclusion process with open boundaries*, J. Stat. Mech. **2006**(12), P12011 (2006), doi:10.1088/1742-5468/2006/12/P12011.

[67] R. A. Blythe and M. R. Evans, *Nonequilibrium steady states of matrix-product form: a solver's guide*, Journal of Physics A: Mathematical and Theoretical **40**(46), R333 (2007), doi:10.1088/1751-8113/40/46/R01.

[68] J. de Gier and F. H. L. Essler, *Slowest relaxation mode of the partially asymmetric exclusion process with open boundaries*, J. Phys. A: Math. Theor. **41**(48), 485002 (2008), doi:10.1088/1751-8113/41/48/485002.

[69] D. Simon, *Construction of a coordinate bethe ansatz for the asymmetric simple exclusion process with open boundaries*, J. Stat. Mech. **2009**(07), P07017 (2009), doi:10.1088/1742-5468/2009/07/p07017.

[70] J. de Gier and F. H. L. Essler, *Large deviation function for the current in the open asymmetric simple exclusion process*, Phys. Rev. Lett. **107**, 010602 (2011), doi:10.1103/PhysRevLett.107.010602.

[71] A. Lazarescu and V. Pasquier, *Bethe Ansatz and Q-operator for the open ASEP*, J. Phys. **A 47**(29), 295202 (2014), doi:10.1088/1751-8113/47/29/295202.

[72] J. Krug, *Boundary-induced phase transitions in driven diffusive systems*, Phys. Rev. Lett. **67**, 1882 (1991), doi:10.1103/PhysRevLett.67.1882.

[73] M. Henkel and G. Schütz, *Boundary-induced phase transitions in equilibrium and non-equilibrium systems*, Physica A: Statistical Mechanics and its Applications **206**(1-2), 187 (1994), doi:10.1016/0378-4371(94)90124-4.

[74] X. Mi, M. Sonner, M. Y. Niu, K. W. Lee, B. Foxen, R. Acharya, I. Aleiner, T. I. Andersen, F. Arute, K. Arya *et al.*, *Noise-resilient edge modes on a chain of superconducting qubits*, Science **378**(6621), 785 (2022), doi:10.1126/science.abq5769.